Journal of the Korean Nuclear Society
Volume 28, Number 2, April 1996

Measurements of Turbulent Flow in a 6×6 Rod Bundle with Spacer Grids

Sun Kyu Yang and Moon Ki Chung
Korea Atomic Energy Research Institute
(Received October 5, 1995)

지지격자를 갖는 6×6 봉다발에서의 난류유동 측정

양선규 · 정문기
한국원자력연구소
(1995. 10. 5 접수)

Abstract

The local hydraulic characteristics in a single phase flow of a 6×6 rod bundle with neighboring different spacer grids were measured by using a LDV(Laser Doppler Velocimeter) system. 6×6 rod bundle is formed by two 3×6 rod bundles with different spacer grids. The objective of this study in a rod bundle is to investigate the thermal-hydraulic interactions between different spacer grids with different configurations and resistance. By using a LDV system, the velocity and turbulent intensity in axial and horizontal directions were measured. Pressure drop measurements were also performed to evaluate the loss coefficient for the spacer grid and the friction factor for rod bundles. Implications concerning thermal mixing due to spacer grids were investigated based on the hydraulic test results. Swirl factor, which is assumed as a qualitative criteria for DNB(departure from nucleate boiling), was defined and estimated from the horizontal velocity results.

요 약

서로 다른 지지격자들이 인접한 6×6 핵연료 봉다발부수로내에서 국부 수력특성인자들을 레이저 유속 측정장치인 LDV(Laser Doppler Velocimeter)를 이용하여 측정하였다. 6×6 봉다발은 서로 다른 지지격자를 가진 3×6 봉다발이 서로 인접하여 이룬 형상이다. 본 연구에서는 다른 형상과 다른 수력저항을 갖는 지지격자간들의 열수력적 상호작용을 규명하는데 그 목적이 있다. LDV를 이용하여 축방향및 횡방향 속도, 난류강도등의 측정인자들을 측정하였다. 또한 압력강하를 측정하여 지지격자의 손실계수와 봉다발의 마찰계수를 구하였다. 수력실험결과에 근거하여 지지격자에 기인된 열혼합현상에 관한것을 연구하였다. DNB의 정성적인 기준이라고 할 수 있는 swirl인자를 정의하고 횡방향속도 실험인자로부터 구하였다.

1. Introduction

In a nuclear fuel design field, the spacer grids in rod bundles are being developed to enhance the thermal mixing efficiency of the coolant flowing through the fuel assembly. However, when the fuel assembly with the newly designed spacer grid is loaded in a reactor, the thermal-hydraulic compatibility between the newly loaded and the existing assemblies is one of the major problems concerned by the nuclear fuel designer. In order to tackle this subject, we performed the experiments by a 6×6 rod bundle with neighboring different spacer grids with different configurations and resistance. 6×6 rod bundle is a combined type with two 3×6 rod bundles with different spacer grids. Literatures for the test of the rod bundle with a mixed spacer grid reported in public are scarce, while those for the test of the rod bundle without or with a spacer grid with uniform resistance can be met frequently in public domain.

Rowe *et al.*[1], Carajilescov and Todreas[2], Renksizbulut and Hadaller[3] and Vonka[4] performed experimental studies on bare rod bundles using laser-Doppler velocimeter(LDV)[5, 6]. Rowe *et al.*, in one of the earliest applications of LDV to subchannel flows, measured turbulent microscopic structures that were helpful in obtaining a better understanding of crossflow mixing between neighboring subchannels. Their results showed that rod gap spacing is the most significant geometric parameter affecting the flow structure. Decreasing the rod gap spacing increases the turbulence intensity, the longitudinal macroscale, and the dominant frequency of turbulence. From the evaluation of the dominant frequency of turbulence, they suggested the presence of periodic flow pulsations in the gap region. Carajilescov and Todreas measured the distributions of axial velocity, turbulence kinetic energy, and Reynolds stresses using a LDV in a simulated interior subchannel of a triangular rod array with $P/D=1.123$ and $x/Dh=77$. Renksizbulut and Hadaller used a square array with $P/D=1.15$. Turbulent mean velocity, intensities, and wall shear stress were measured using a LDV and calibrated Preston tube. They suggested the probable presence of secondary flows in the corner from the results of the skewed wall shear stress profiles and deformed constant-velocity lines. Secondary flows were investigated by Vonka. He explained that secondary flows of relatively low magnitude are superimposed on a main or primary flow and cause the flow to spiral through the passage.

In this study, the detailed hydraulic characteristics of the turbulent flow in subchannels of a 6×6 rod bundle with neighboring different spacer grids were measured by using a LDV. The measured parameters include the velocity and turbulent intensity in axial and horizontal directions. Pressure drops were also measured to estimate loss coefficients for the spacer grid and friction factors for rod bundles. Thermal mixing in rod bundles was studied based on the hydraulic test results. Swirl factor, which is assumed as a qualitative criteria for DNB(departure from nucleate boiling), was defined and estimated from the horizontal velocity results.

2. Experimental Method

The tested 6×6 spacer grid is shown in Fig. 1 with major dimensions. 6×6 spacer grid is a combined type formed by two different 3×6 spacer grids with different configurations and resistance. One of them is a spacer grid with mixing vanes. Mixing vanes are attached on the spacer grid with an angle of 22°. The cross-section of 81mm square housing consists of 36 rods of 9.5mm in diameter as shown in Fig. 2. The rod bundle forms in a square array. The hydraulic diameter(D_h) of the entire channel is 11.468mm. Axial locations of spacer grids and pressure taps together with a coordinate system are shown in Fig. 3. Water is the working fluid and flows upward. Test section is set up in test-loop shown schematically in Fig. 4, which includes variable speed pump, a storage tank, flow control values, and turbine flow meters etc. During the experiments, the water tem-

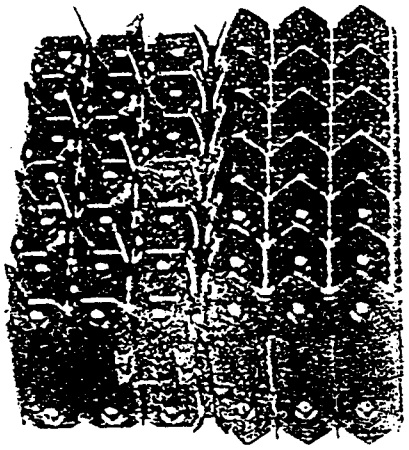

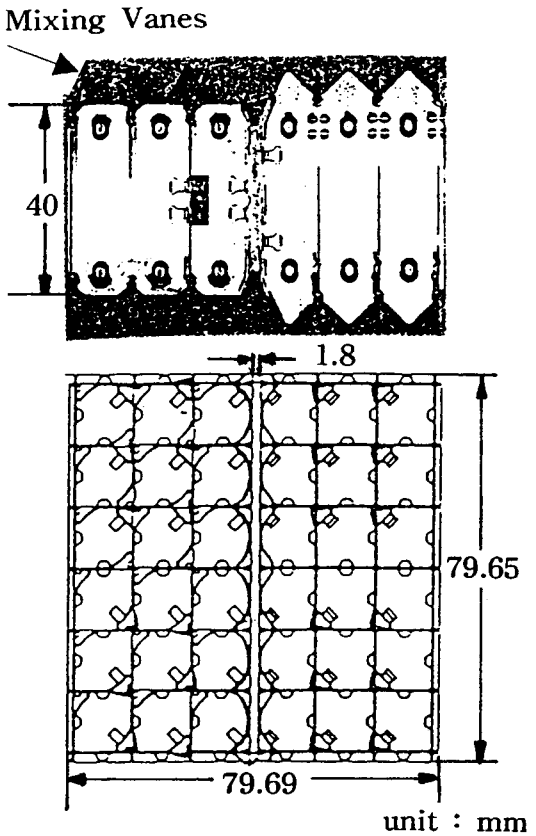

Fig. 1. 6×6 Spacer Grid Combined by Mixing Vaned and Straight Types

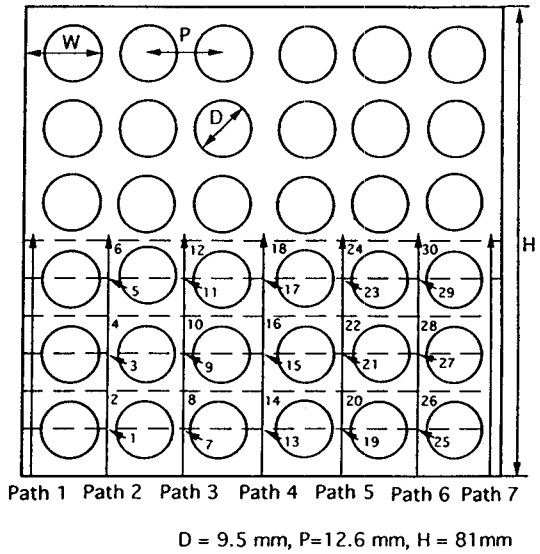

Fig. 2. Cross-section of 6×6 Rod Bundles Showing the Measuring Locations

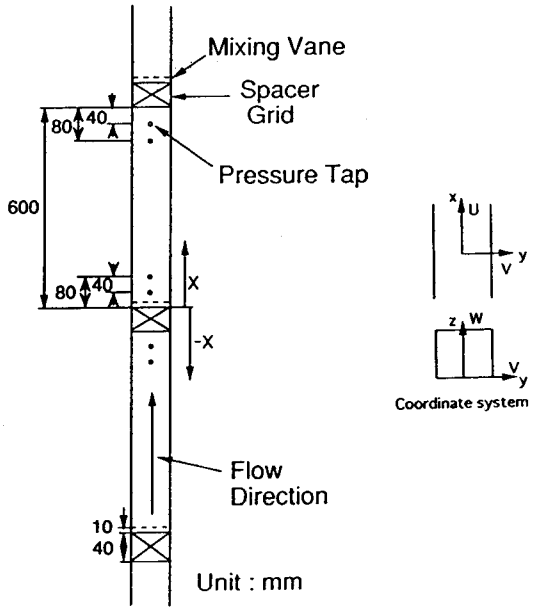

Fig. 3. Axial Locations of Spacer Grids and Pressure Taps

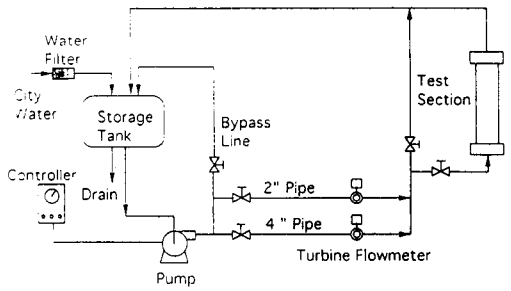

Fig. 4. Schematic Diagram of Test Loop

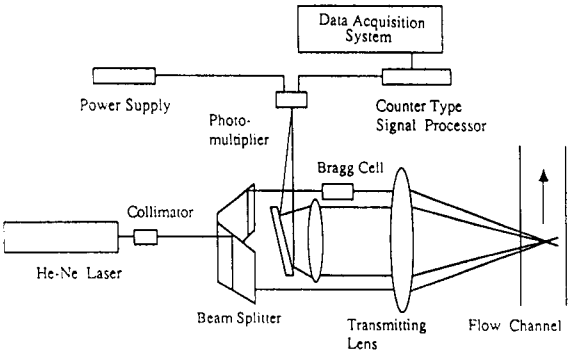

Fig. 5. Backward Scattered Mode of LDV System

perature in the test section was maintained at 25°C by adjusting the feed and drain of water in the storage tank. The flow rate was 20kg/sec resulting in an average flow velocity of 5m/sec and a Reynolds number based on the hydraulic diameter of Re=63924. The square housing is made of acrylic to allow access for laser beams to the location where the velocity measurement is to be performed.

The one-component He-Ne LDV system from TSI used in the present work was aligned by the dual-beam backward scattered mode as shown in Fig. 5. The dual beam spacing is 50mm and the focal-length of the focusing lens is 350mm. Silicon carbide particles, 1.5μm in diameter, 3.2g/cm^3 in density, 2.65 in refractive index, and 1.4 in geometrical standard deviation, were added into the fluid to obtain the scattered signal. The signals from the photomultiplier were processed using a counter type processor which consists of filters, an amplifier, a timer, a digital output, and a D/A(Digital to Analog) converter. The signals from the digital output of the signal processor were used to obtain the turbulent velocity and intensity by using data analysis program FIND from TSI installed in a personal computer. In this software, the correcting process for velocity bias is included. In order to detect negative velocity in horizontal direction, Bragg cell was added in the LDV alignment. Axail and horizontal velocities were measured independently by adjusting alignment angle.

Measuring paths and locations are shown in Fig. 2. Turbulent velocities were measured at Paths 1~7 with varying the axial locations. In the present test section, since flow region is not symmetric, Paths are covering whole flow subchannels, and located at central region in gap between rod bundles. Points 1~30 are indicated for representations of the turbulence decay behind the spacer grid in Section 3. Pressure drops were measured at pressure taps shown in Fig. 3.

3. Results and Discussions

3.1. Pressure Drops

Loss coefficients(C_B) for the spacer grid and friction factors for the rod bundles were obtained from the measured pressure drops[7, 8]. Fig. 6 shows the loss coefficient profile with variation of Reynolds

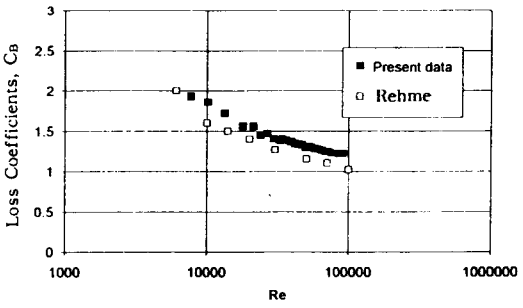

Fig. 6. Loss Coefficients for the 6×6 Spacer Grid

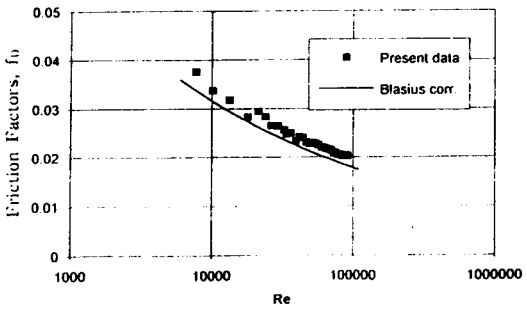

Fig. 7. Friction Factors for the 6×6 Rod Bundles

number based on hydraulic diameter and average velocity. Loss coefficients are compared with the reproduced Rehme[7]'s data for the square array with the spacer grid of tube squares axially connected. The present data show higher values than those reported by Rehme. The friction factors(f) in rod bundles were estimated as shown in Fig. 7. and compared with the Blasius[9] correlation. The results show that those of the present work are a litle higher, than the values given by the Blasius curve.

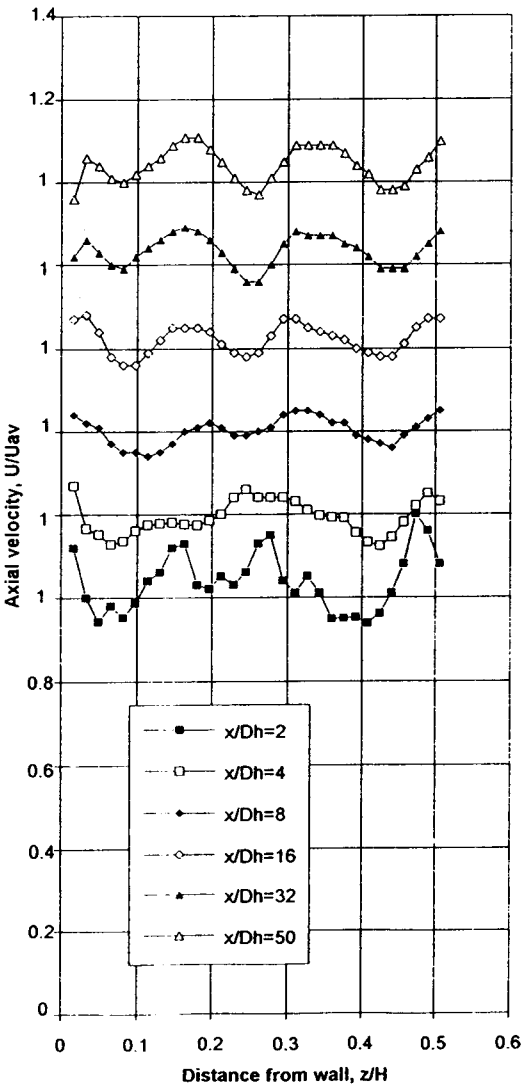

Fig. 8. Developing Axial Velocity at Path 3

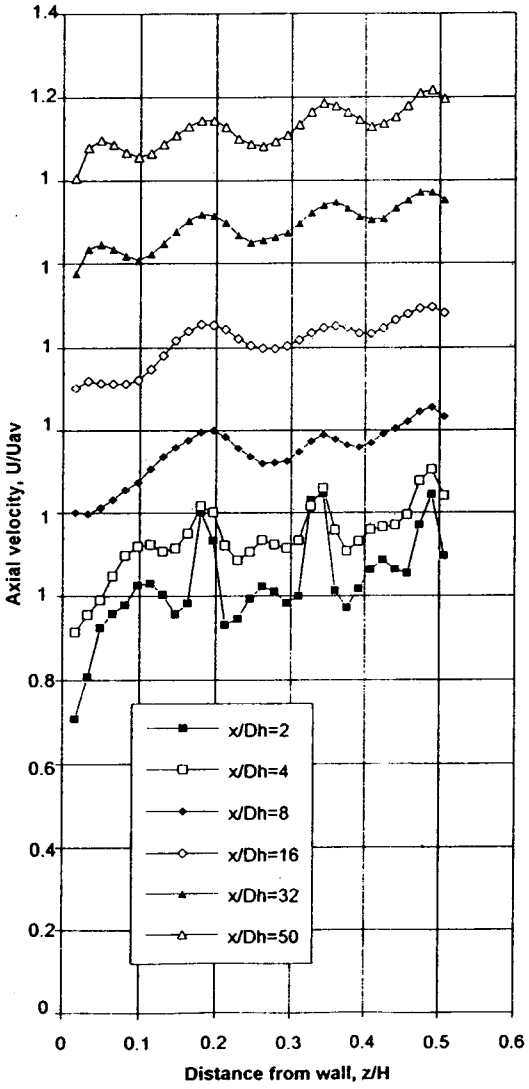

Fig. 9. Developing Axial Velocity at Path 4

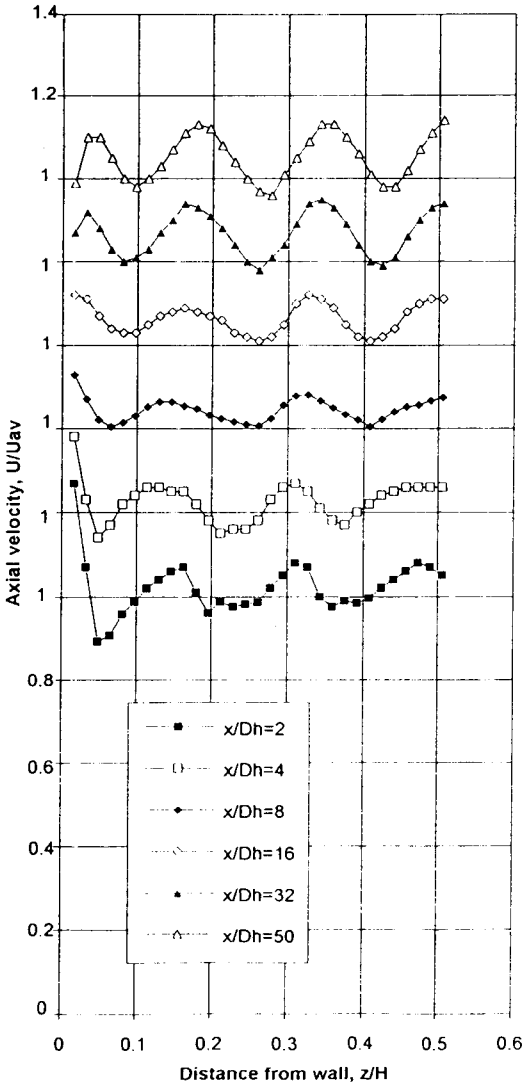

Fig. 10. Developing Axial Velocity at Path 5

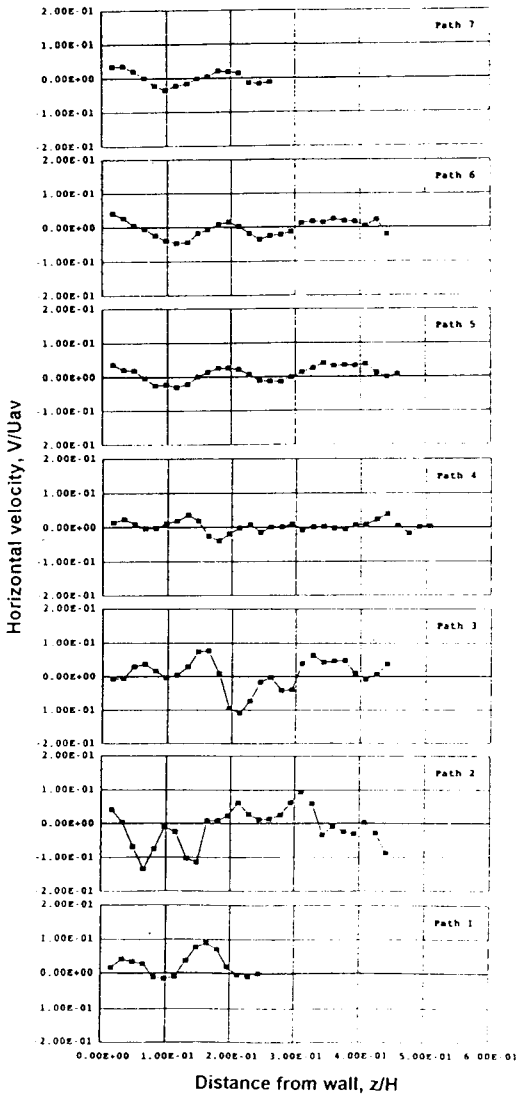

Fig. 11. Horizontal Velocity Profiles at $x/D_h=1$

3.2. Velocity Profiles

Figs. 8~10 show the developing axial velocity profiles at Paths 3~5. The lower spacer grids disturb the local velocity field, which causes a change in mass flow within each subchannel through the spacer grids. Near spacer grid, at $x/D_h=2$, the flow fluctuates drastically due to the flow blockage and turbulence generation induced by the sharp edge of the spacer grid. At $x/D_h=50$, the flow is nearly developed. The velocity profiles at Path 4, which is along the central gap between different spacers, are different from the others. This is due to that the flow at this gap is not disturbed by any obstacles.

Horizontal velocities at diferent axial locations are shown in Figs. 11~14. Horizontal velocities at $x/D_h=1$ are fluctuating intensively in particular at Paths 1~3. This implies that the mixing vaned spacer grid generates higher turbulence. The inconsistent data points in numbers at Paths are caused from

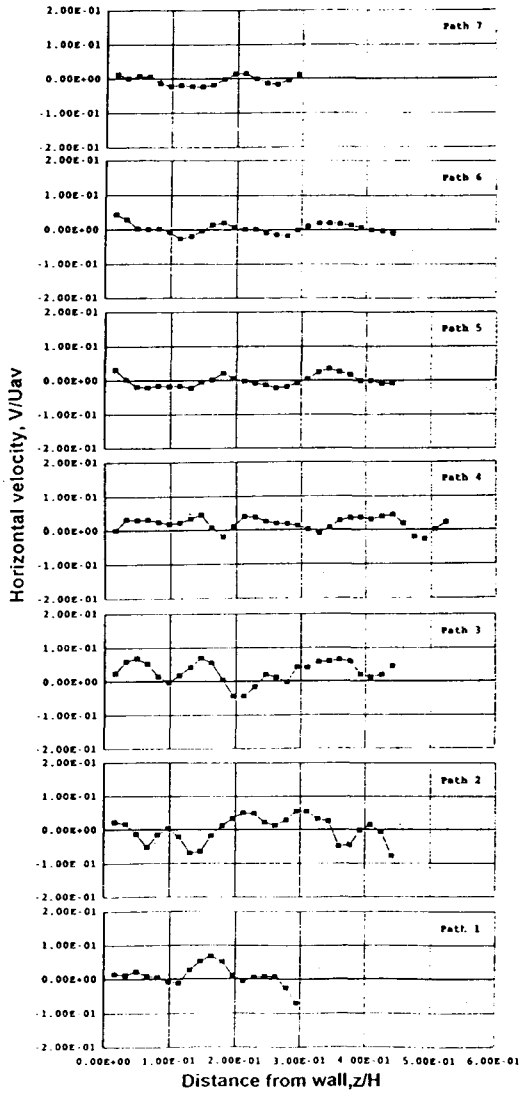

Fig. 12. Horizontal Velocity Profiles at $x/D_h=2$

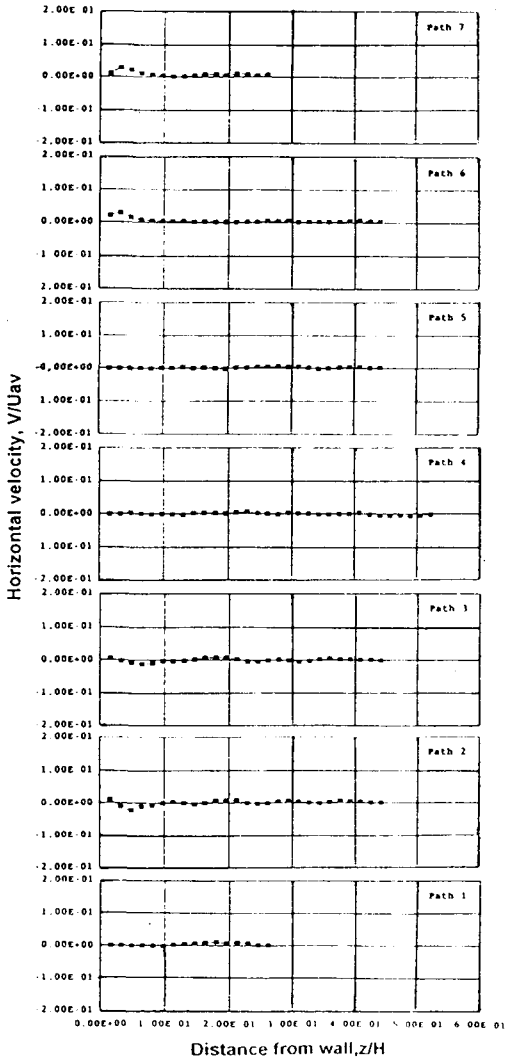

Fig. 13. Horizontal Velocity Profiles at $x/D_h=50$

beam blockade by rod bundles or housing wall. Two beams are going through test section in parallel for measuring the horizontal velocity. In some distance, beams are touched with the housing wall or the surface of rods arranged closely. The maximum local horizontal velocity is shown at Path 2, $x/D_h=1$, as -0.675m/sec. As the flow develops, horizontal velocities become smaller to nearly zero. In Fig. 13 for $x/D_h=50$, the horizontal velocities do not vanished near wall at some Paths. This implies that the flow is not fully developed locally in the grid span. Fig. 14 represents horizontal velocities at different axial locations at gap between different spacer grids. The highest average horizontal velocity at Path 4 is observed at $x/D_h=2$, whose magnitude is 0.1m/sec. It should be noted that the highest velocity is not found at $x/D_h=1$ but $x/D_h=2$. This can be explained by the enertia force of the flow leaving the leading edge of the spacer grid in the gap between different spacer grids.

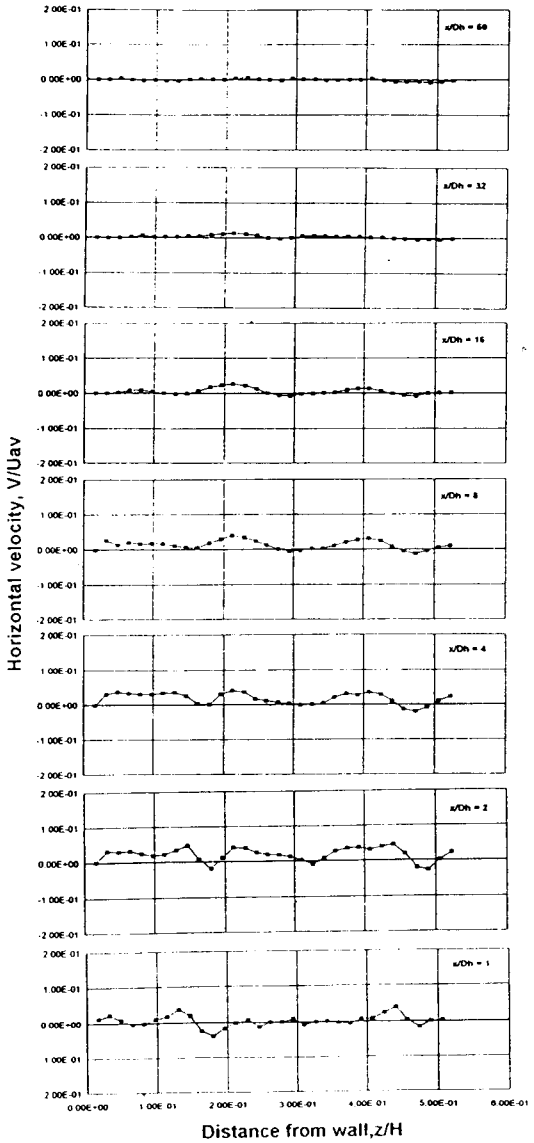

Fig. 14. Horizontal Velocity Profiles at Path 4

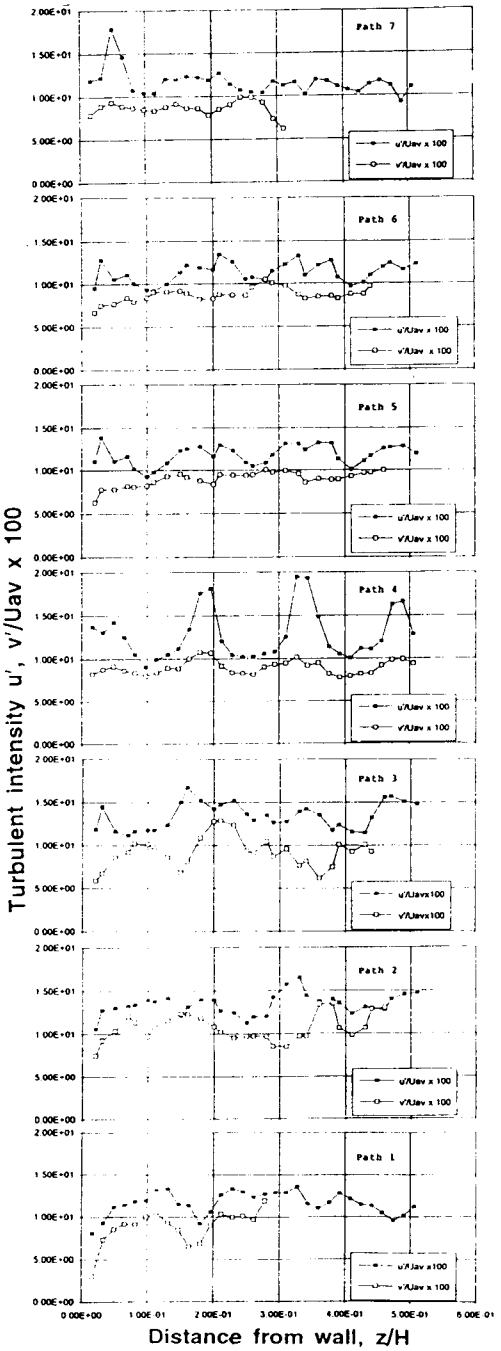

Fig. 15. Turbulent Intensity at x/D_h=2

3.3. Turbulent Intensity

Figs. 15~16 represent axial and horizontal turbulent intensity profiles at different axial levels. The highest intensity is distributed at $x/D_h=2$ near the lower spacer grid. The turbulent intensity increases drastically through spacer grids, and then decreases rapidly to the stable level as the flow is developing. The intensities decrease to the lowest value at $x/D_h=32$ and 50. Horizontal turbulent intensities show lower values than axial ones. Above $x/D_h=32$, the turbu-

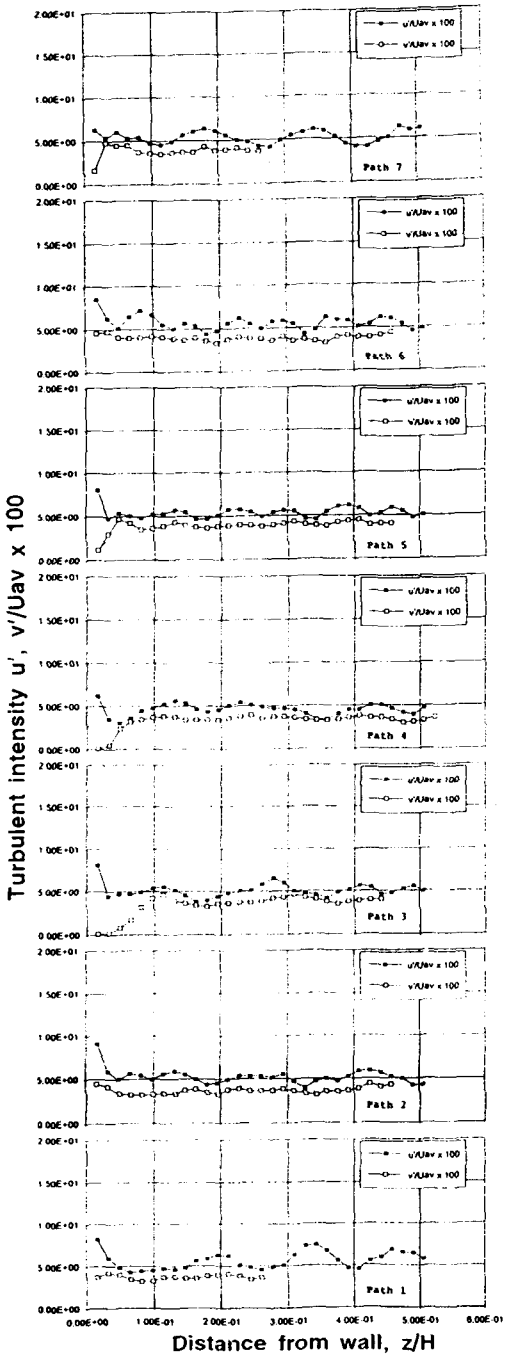

Fig. 16. Turbulent Intensity at x/D_h=32

lent intensity distributions are nearly fully developed. Behind the spacer grid, mixing vaned spacer grid generates higher turbulence than that without mixing vanes. In Table 1, averages of axial and horizontal turbulent intensities at x/D_h=2 are tabulated. The values at Paths 2 and 3 in the mixing vaned spacer grid region show higher magnitude than those at Paths 5 and 6. This implies that the mixing vaned spacer grid generates higher turbulence.

Table 1. Average of u' and v' at x/D_h=2 Along Paths

	Path 2	Path 3	Path 4	Path 5	Path 6
Aver. of u′ (m/sec)	0.671	0.67	0.638	0.588	0.564
Aver. of v′ (m/sec)	0.535	0.458	0.465	0.448	0.433

3.4. Thermal Mixing in Rod Bundles

Thermal hydraulic behavior of the fluid at the spacer grid is hard to analyze in detail due to the complex geometry. Unal et al.[10] measured the pressure drops at rod bundles spacer grid for the post-CHF condition. However, the evaluation of the experimental results was mentioned not to be easy because of the diffculty in prediction of the complex thermal hydraulic phenomena at the spacer grid. It has been reasonably suggested [11] that more detailed descriptions for the single phase flow be needed for a better understanding of the multiphase flows. In a possible way to approach this problem, the relation between heat and momentum transfer in turbulent flow can give information on the thermal behavior near spacer grid. Yao et al.[12] studied heat transfer augmentation by straight grid spacers in rod bundles. For single phase flow and for post-critical heat flux dispersed flow, the local heat transfer at a straight spacer and its upstream and downstream locations were treated. The highest local heat transfer is observed near the spacer grid, and downstream of the spacer grid, the heat transfer augmentation rapidly decays with x/D_h exponentially. In the present study, some quantitative values of thermal mixing due to

turbulence and convective flow swirling were evaluated as follows.

3.4.1. Heat Transfer Due to the Turbulent Mixing

The mixing factor related to the turbulent mixing was obtained from the measured turbulent parameter by imploying Yang and Chung's method[8]. In Fig. 17, local mixing factors, Y, were obtained at Paths 3~5. Mixing factors show the higest values near the spacer grid and they decrease rapidly up to about $x/D_h=15$. After $x/D_h=15$, the stable values are observed. However, slight increasing is found at Paths 4 and 5 after $x/D_h=15$. This increasing of the mixing factor is caused by the turbulence increase which was also observed for the 5×5 rod bundle test in Ref. 8.

3.4.2. Heat Transfer Due to the Convective Swirling

Following the analogy of heat and momentum transfer, convective heat transfer correlation in rod bundles with spacer grids is obtained[12]. The ratio of the pressure drops in rod bundles with and without the spacer grid is

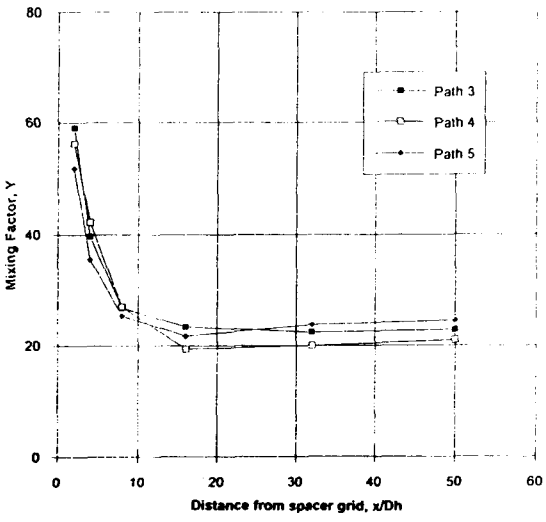

Fig. 17. Mixing Factors at Paths 3~5

$$\left(\frac{\Delta P}{\Delta P_o}\right)=\frac{f+C_B\frac{D_h}{L}}{f}=1+\frac{D_h}{fL}C_B \quad (1)$$

where f is the friction factor without spacer grids and C_B is the loss coefficients which can be given by a blockage ratio

$$C_B=C_v\,\beta^2 \quad (2)$$

Here β and C_v are a blockage ratio and a modified loss coefficient, respectively. The blockage ratio is the ratio of the projection area of spacer grid and mixing vanes to the flow area of the entire subchannel in axial direction. Marek and Rehme[13] suggested the heat transfer augmentation at straight spacer grids on smooth rods in a sigle phase flow by correlating pressure drop data and considering the analogy between heat and momentum transfer.

$$\frac{Nu}{Nu_o}=1+5.55\beta^2 \quad (3)$$

where Nuo is the Nusselt number for rod bundles without spacer grids. Yao *et al.*[12] extended the local Nusselt number correlation up to the downstream region behind the spacer grid with mixing vanes as

$$\frac{Nu}{Nu_o}=\left[\ 1+5.55\beta^2 e^{-0.13(x/D_h)}\right]$$

$$\left[\ 1+A^2\tan^2\phi e^{-0.034(x/D_h)}\right]^{0.4} \quad (4)$$

for the downstream region for single phase flow. This equation is valid for the vane angles less than 45 deg.

In this work, swirl factor is defined as

$$Sw_{(x/D_h)}=\frac{1}{L}\int\frac{|V|}{U}\,dz \quad (5)$$

where

L : length of integral path

V : lateral velocity at measurement location perpendicular to the integral path

U : axial velocity at measurement location

Fig. 18 shows the swirling rotations generated by the mixing vaned spacer grid. The mgnitude of swirl

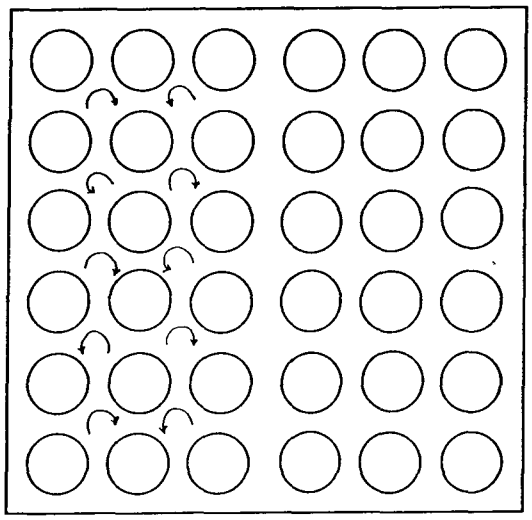

Fig. 18. Swirling Roation in Subchannels

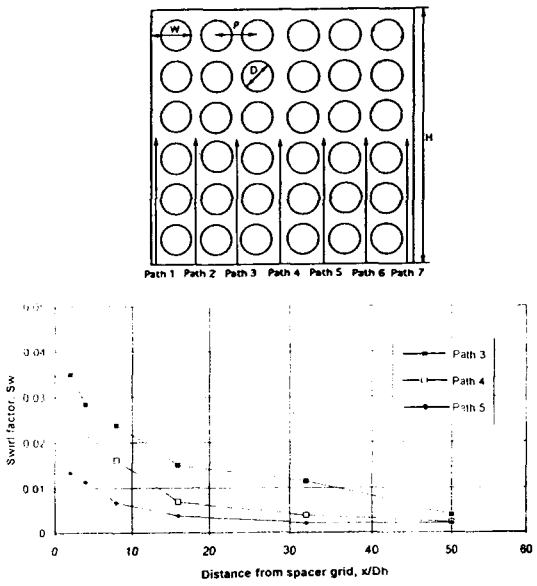

Fig. 19. Local Swirling Factor in Axial Variations

factor is assumed to be a qualitative indicator of the spacer design on DNB(departure from nucleate boiling) performance[14]. Swirl factors were estimated from the measured horizontal velocities as shown in Fig. 19. In axial variations, swirl factors are plotted for the different Paths. Higher swirling are indicated in the mixing vaned spacer grid region. By this swirl factor, Eq.(4) can be written as

$$\frac{Nu}{Nu_o} = [\ 1+5.55\beta^2 e^{-0.13(x/D_h)}]\ [\ 1+Sw^2_{(x/D_h)}]^{0.4} \qquad (6)$$

The heat transfer predictions for the present case were performed by using the experimental data. In obtaining Nusselt numbers, Eq.(6) was used instead of Eq.(4), since swirl factor was directly obtained by Eq.(5) using the experimental results. In 6×6 rod bunles, two different types of spacer grids are combined with different blockage ratios, 0.3 for the mixing vaned spacer grid and 0.214 for the straight spacer grid. In calculations at Paths 3 and 5, blockage ratios are used their own values differently. In Fig. 20, the predicted local Nusselt numbers for the present case are plotted and compared with those by Yao *et al.* for a blockage ratio of 0.328, and swirl factors of 0. 57 and 1.0 at the inlet. As shown in Fig. 20, the coolant thermal efficiency of the mixing vaned spacer grid is higher than that of the straight spacer grid. In this case, the blockage ratios of the spacer grids are more influential in heat transfer phenomena of rod bundles.

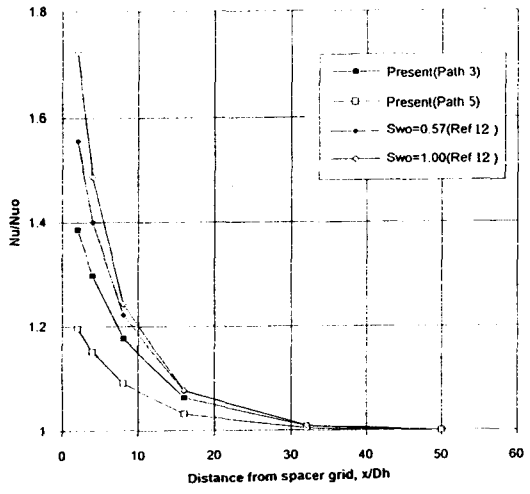

Fig. 20. Nusselt Numbers in Axial Variations

Table 2. Uncertainty Values

Parameter	Norminal Value	Uncertainty Values	
		Value	Persent(%)
Axial Mean Velocity, U	5.07 m/s	0.15 m/s	± 3
Horizontal Mean Velocity, V	0.5 m/s	0.015 m/s	± 3
Turbulent Intensity, u′/U, v′/U	0.043	0.00258	± 6
Axial Location, x		± 0.1mm	
Transverse Location, y, z		± 0.005mm	

3.5. Uncertainty Analysis

An Uncertainty analysis was performed to estimate data accuracy by the error and uncertainty methods of Moffat[15]. Table 2 is a summary of the uncertainty analysis.

4. Concluding Remarks

Measurements of turbulent flow in subchannels of a 6×6 rod bundle with neighboring different spacer grids were performed by using a LDV(laser Doppler velocimeter). Pressure drops were also measured to estimate the loss coefficients for the spacer grid and the friction factors for the rod bundles. The experimental results led to the following conclusions.

The friction factors for the 6×6 rod bundle show a little higher values than those given by the Blasius curve. The maximum local horizontal velocity is found at Path 2, $x/D_h=1$, as -0.675 m/sec. The highest average horizontal velocity in the gap between the different spacer grids is 0.1m/sec which is observed at $x/D_h=2$. Thermal mixing in rod bundles with spacer grids was discussed based on the hydraulic test results. Quantitative correlations of thermal mixing due to turbulence and convective swirling were estimated from the measured data. Mixing vaned spacer grid generates higher turbulence and thermal mixing than that without mixing vanes.

Acknowledgements

The bundle tested in this study was assembled with Zircaloy tubes obtained from KNFC and spacer grids of Siemens type provided by Nuclear Fuel Design Group at KAERI. The authors wish to express their appreciation to them.

Nomenclatures

C_B loss coefficient
C_v modified loss coefficient
D rod diameter, m
D_h hydraulic diameter, m
friction factor
Nu Nusselt number
Nu_∞ Nusselt number far downstream
P pitch, m
P pressure, Pa
Re Reynolds number $(U_{av} D_h/v)$, dimensionless
s rod gap spacing, m
U axial time mean velocity, m/s
U_{av} entire subchannel average velocity, m/s
u axial fluctuating velocity, m/s
u' root mean square of u, m/s
V radial time mean velocity, m/s
v radial fluctuating velocity, m/s
x axial coordinate, m
Y mixing factor
y lateral coordinate, m
z azimuthal coordinate, m

Greek Symbols

β blockage ratio
ν kinematic viscosity, m^2/s

References

1. D.S. Rowe, B.M. Johnson, and J. G. Knudsen, "Implications Concerning Rod Bundle Cross-flow Mixing Based on Measurements of Turbulent Flow Structure," *Int. J. Heat Mass Transfer*, 17, 407~418 (1974)
2. P. Carajilescov and N.E. Todreas, "Experimental and Analytical Study of Axial Turbulent Flows in an Interier Subchannel of a Bare Rod Bundle," *J. Heat Transfer, Trans. ASME*, 101, 354~363 (1979)
3. M. Renksizbulut and G. I. Hadaller, "An Experimental Study of Turbulent Flow through a Square Array Rod Bundles," *Nucl. Eng. Des.*, 91, 41~55 (1986)
4. V. Vonka, "Measurement of Secondary Flow Vortices in a Rod Bundle," *Nucl. Eng. Des.*, 106, 191~207 (1988)
5. F. Durst, A. Melling and J.H. Whitelaw, Principles and Practice of Laser Doppler Anemometry, Academic Press (1976)
6. L.E. Drain, The Laser Doppler Technique, John Wiley and Sons (1980)
7. K. Rehme, "Pressure Drop Correlation for Fuel Element Spacers," *Nucl. Technol. Vol.* 17, 15~23 (1973)
8. S.K. Yang and M.K. Chung, "Turbulent Flow through Mixing Spacer Grids in Rod Bundles, " HTD-Vol. 316, National Heat Transfer Conference, ASME, Vol. 14, 33~40 (1995)
9. H. Blasius, The Law of Similarity for Frictional Processes in Fluids (originally in German), Forsch Arb. Ing. -Wesen(Berlin) (1913)
10. C. Unal, O. Badr, K. Tuzla, J.C. Chen, and S. Neti, "Pressure Drop at Rod-Bundle Spacers in the Post-CHF Dispersed Flow Regime," *Int. J. Multiphase Flow*, Vol. 20, No. 3, pp. 515~522 (1994)
11. F. de Crecy, and D. Juhel, "Methodology of Study of the Boiling Crisis in a Nuclear Fuel Rod Bundle," NURETH-7, Saratoga Springs, New York, Sep. 10~15, NUREG/CP-0142, Vol. 4, 2480~2488 (1995)
12. S.C. Yao, L.E. Hochreiter and W.J. Leech, "Heat Transfer Augmentation in Rod bundles near Grids," *J. of Heat Transfer, Trans. of the ASME*, Vol. 104, 76~81 (1982)
13. J. Marek and K. Rehme, "Heat Transport in Smooth and Roughened Rod Bundles near Spacer Grids," *Fluid Flow and Heat Transfer over Rod or Tube Bundles*, Ed. by S. Yao and P. Pfund, ASME, 163-170 (1979)
14. Z. Karoutas, C-Y Gu, and B. Scholin, "3-D Flow Analyses for Design of Nuclear Fuel Spacer," NURETH-7, Saratoga Springs, New York, Sep. 10~15, *NUREG/CP-0142*, Vol. 4, 3153~3174 (1995)
15. R.J. Moffat, "Describing the Uncertainty in Experimental Results," *Exp. Thermal Fluid Science*, Vol. 1, 3~17 (1988)